Proof. This is a slightly sharpened version of Theorem 3.5 in Isaacson and Keller (1966), and is easily proved along the same lines. □

When the tridiagonal matrix results from application of a block iterative method to a system of which the matrix is a K-matrix, the conditions Theorem 4.3.1 are satisfied.

Vectorized and parallel computing

The basic iterative methods discussed above differ in their suitability for computing with vector or parallel machines. Since the updated quantities are mutually independent, Jacobi parallizes and vectorizes completely, with vector length $I*J$. If the structure of the stencil [**A**] is as in Figure 3.4.2(c), then with zebra Gauss–Seidel the updated blocks are mutually independent, and can be handled simultaneously on a vector or a parallel machine. The same is true for point Gauss–Seidel if one chooses a suitable four-colour ordering scheme. The vector length for horizontal or vertical zebra Gauss–Seidel is J or I, respectively. The white and black groups in white–black Gauss–Seidel are mutually independent if the structure of [**A**] is given by Figure 4.3.3. The vector length is $I*J/2$. With diagonal Gauss–Seidel, the points inside a diagonal are mutually independent if the structure of [**A**] is given by Figure 3.4.2(b), if the diagonals are chosen as in Figure 4.3.1. The same is true when [**A**] has the structure given in Figure 3.4.2(a), if the diagonals are rotated by 90°. The average vector length is roughly $I/2$ or $J/2$, depending on the length of largest the diagonal in the grid. With Gauss–Seidel–Jacobi lines in the grid can be handled in parallel; for example, with the forward ordering of Figure 4.3.1 the points on vertical lines can be updated in parallel, resulting in a vector length J. In white–black line Gauss–Seidel points of the same colour can be updated simultaneously, resulting in a vector length of $I/2$ or $J/2$, as the case may be.

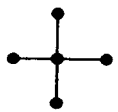

Figure 4.3.3 Five-point stencil.

Exercise 4.3.1. Let $\mathbf{A} = \mathbf{L} + \mathbf{D} + \mathbf{U}$, with $l_{ij} = 0$ for $j \geqslant i$, $\mathbf{D} = \text{diag}(\mathbf{A})$, and $u_{ij} = 0$ for $j \leqslant i$. Show that the iteration matrix of symmetric point Gauss–Seidel is given by

$$\mathbf{S} = (\mathbf{U} + \mathbf{D})^{-1}\mathbf{L}(\mathbf{L} + \mathbf{D})^{-1}\mathbf{U} \tag{4.3.11}$$

Exercise 4.3.2. Prove Theorem 4.3.1.

4.4. Examples of basic iterative methods: incomplete point LU factorization

Complete LU factorization

When solving $Ay = b$ directly, a factorization $\mathbf{A} = \mathbf{LU}$ is constructed, with **L** and **U** a lower and an upper triangular matrix. This we call *complete factorization*. When **A** represents a discrete operator with stencil structure, for example, as in Figure 3.4.2, then **L** and **U** turn out to be much less sparse than **A**, which renders this method inefficient for the class of problems under consideration.

Incomplete point factorization

With *incomplete factorization* or *incomplete* **LU** *factorization* (**ILU**) one generates a splitting $\mathbf{A} = \mathbf{M} - \mathbf{N}$ with **M** having sparse and easy to compute lower and upper triangular factors **L** and **U**:

$$\mathbf{M} = \mathbf{LU} \tag{4.4.1}$$

If **A** is symmetric one chooses a symmetric factorization:

$$\mathbf{M} = \mathbf{LL}^{\mathrm{T}} \tag{4.4.2}$$

An alternative factorization of **M** is

$$\mathbf{M} = \mathbf{LD}^{-1}\mathbf{U} \tag{4.4.3}$$

With *incomplete point factorization*, **D** is chosen to be a diagonal matrix, and $\text{diag}(\mathbf{L}) = \text{diag}(\mathbf{U}) = \mathbf{D}$, so that (4.4.3) and (4.4.1) are equivalent. **L**, **D** and **U** are determined as follows. A *graph* $\mathcal{G}$ of the incomplete decomposition is defined, consisting of two-tuples (i, j) for which the elements l_{ij}, d_{ii} and u_{ij} are allowed to be non-zero. Then **L**, **D** and **U** are defined by

$$(\mathbf{LD}^{-1}\mathbf{U})_{kl} = a_{kl}, \quad \forall (k, l) \in \mathcal{G} \tag{4.4.4}$$

We will discuss a few variants of ILU factorization. These result in a splitting $\mathbf{A} = \mathbf{M} - \mathbf{N}$ with $\mathbf{M} = \mathbf{LD}^{-1}\mathbf{U}$. *Modified incomplete point factorization* is obtained if **D** as defined by (4.4.4) is changed to $\mathbf{D} + \sigma\tilde{\mathbf{D}}$, with $\sigma \in \mathbb{R}$ a parameter, and $\tilde{\mathbf{D}}$ a diagonal matrix defined by $\tilde{d}_{kk} = \Sigma_{l \neq k} \mid n_{kl} \mid$. From now on the modified version will be discussed, since the unmodified version follows as a special case. This or similar modifications have been investigated in the context of multigrid methods by Hemker (1980), Oertel and Stüben (1989), Khalil (1989, 1989a) and Wittum (1989a, 1989c). We will discuss a few variants of modified ILU factorization.

Five-point ILU

Let the grid be given by (4.3.1), let the grid points be ordered according to (4.3.2), and let the structure of the stencil be given by Figure 4.3.3. Then the graph of **A** is

$$\mathcal{G} = \{(k, k-I), (k, k-1), (k, k), (k, k+1), (k, k+I)\} \tag{4.4.5}$$

For brevity the following notation is introduced

$$a_k = a_{k,k-I}, \quad c_k = a_{k,k-1}, \quad d_k = a_{kk}, \quad q_k = a_{k,k+1}, \quad g_k = a_{k,k+I} \tag{4.4.6}$$

Let the graph of the incomplete factorization be given by (4.4.5), and let the non-zero elements of **L**, **D** and **U** be called α_k, γ_k, δ_k, μ_k and η_k; the locations of these elements are identical to those of $a_k, \ldots, g_k$, respectively. Because the graph contains five elements, the resulting method is called *five-point ILU*. Let $\alpha, \ldots, \eta$ be the $IJ * IJ$ matrices with elements $\alpha_k, \ldots, \eta_k$, respectively, and similarly for $a, \ldots, g$. Then one can write

$$\mathbf{L}\mathbf{D}^{-1}\mathbf{U} = \alpha + \gamma + \delta + \mu + \eta + \alpha\delta^{-1}\mu + \alpha\delta^{-1}\eta + \gamma\delta^{-1}\mu + \gamma\delta^{-1}\eta \tag{4.4.7}$$

From (4.4.4) it follows

$$\alpha = a, \quad \gamma = c, \quad \mu = q, \quad \eta = g \tag{4.4.8}$$

and, introducing modification as described above,

$$\delta + a\delta^{-1}g + c\delta^{-1}g = d + \sigma\tilde{d} \tag{4.4.9}$$

The rest matrix **N** is given by

$$\mathbf{N} = a\delta^{-1}q + c\delta^{-1}g + \sigma\tilde{d} \tag{4.4.10}$$

The only non-zero entries of **N** are

$$\begin{aligned} n_{k,k-I+1} &= a_k\delta_{k-I}^{-1}q_{k-I}, \quad n_{k,k+I-1} = c_k\delta_{k-1}^{-1}g_{k-1} \\ n_{kk} &= \sigma(|\, n_{k,k-I+1}\,| + |\, n_{k,k+I-1}\,|) \end{aligned} \tag{4.4.11}$$

Here and in the following elements in which indices outside the range $[1, IJ]$ occur are to be deleted. From (4.4.9) the following recursion is obtained:

$$\delta_k = d_k - a_k\delta_{k-I}^{-1}g_{k-I} - c_k\delta_{k-1}^{-1}q_{k-1} + n_{kk} \tag{4.4.12}$$

This factorization has been studied by Dupont *et al.* (1968).

From (4.4.12) it follows that δ can overwrite d, so that the only additional storage required is for **N**. When required, the residual $b - \mathbf{A}y^{m+1}$ can be computed as follows without using **A**:

$$b - \mathbf{A}y^{m+1} = \mathbf{N}(y^{m+1} - y^m) \tag{4.4.13}$$

which follows easily from (4.1.3). Since **N** is usually more sparse than **A**, (4.4.13) is a cheap way to compute the residual. For all methods of type (4.1.3) one needs to store only **M** and **N**, and **A** can be overwritten.

Seven-point ILU

The terminology *seven-point ILU* indicates that the graph of the incomplete factorization has seven elements. The graph $\mathcal{G}$ is chosen as follows:

$$\mathcal{G} = \{(k, k \pm I), (k, k \pm I \mp 1), (k, k \pm 1), (k, k)\} \tag{4.4.14}$$

Let the graph of **A** be contained in $\mathcal{G}$. For brevity we write $a_k = a_{k,k-I}$, $b_k = a_{k,k-I+1}$, $c_k = a_{k,k-1}$, $d_k = a_{kk}$, $q_k = a_{k,k+1}$, $f_k = a_{k,k+I-1}$, $g_k = a_{k,k+I}$.

The structure of the stencil associated with the matrix **A** is as in Figure 3.4.2(a). Let the elements of **L**, **D** and **U** be called α_k, β_k, γ_k, δ_k, μ_k, ζ_k and η_k. Their locations are identical to those of $a_k, \ldots, g_k$, respectively. As before, let $\alpha, \ldots, \eta$ and $a, \ldots, g$ be the $IJ * IJ$ matrices with elements $\alpha_k, \ldots, \eta_k$ and $a_k, \ldots, g_k$ respectively. One obtains:

$$\mathbf{L}\mathbf{D}^{-1}\mathbf{U} = \alpha + \beta + \gamma + \delta + \mu + \zeta + \eta + (\alpha + \beta + \gamma)\delta^{-1}(\varepsilon + \zeta + \eta) \tag{4.4.15}$$

From (4.4.4) it follows that, with modification,

$$\begin{aligned} &\alpha = a, \beta + \alpha\delta^{-1}\mu = b, \quad \gamma + \alpha\delta^{-1}\zeta = c \\ &\delta + \alpha\delta^{-1}\eta + \beta\delta^{-1}\zeta + \gamma\delta^{-1}\mu = d + \sigma\tilde{d} \\ &\mu + \beta\delta^{-1}\eta = q, \quad \zeta + \gamma\delta^{-1}\eta = f, \quad \eta = g \end{aligned} \tag{4.4.16}$$

The error matrix $\mathbf{N} = \beta\delta^{-1}\mu + \gamma\delta^{-1}\zeta + \sigma\tilde{d}$ so that its only non-zero elements are

$$\begin{aligned} n_{k,k-I+2} &= \beta_k\delta_{k-I+1}^{-1}\mu_{k-I+1}, \quad n_{k,k+I-2} = \gamma_k\delta_{k-1}^{-1}\zeta_{k-1} \\ \sigma\tilde{d}_k &= n_{kk} = \sigma(|\, n_{k,k-I+2}\,| + |\, n_{k,k+I-2}|) \end{aligned} \tag{4.4.17}$$

From (4.4.16) we obtain the following recursion:

$$\begin{aligned} &\alpha_k = a_k, \quad \beta_k = b_k - a_k\delta_{k-I}^{-1}\mu_{k-I}, \quad \gamma_k = c_k - a_k\delta_{k-I}^{-1}\zeta_{k-I} \\ &\delta_k = d_k - a_k\delta_{k-I}^{-1}g_{k-I} - \beta_k\delta_{k-I+1}^{-1}\zeta_{k-I+1} - \gamma_k\delta_{k-1}^{-1}\mu_{k-1} + n_{kk} \\ &\mu_k = q_k - \beta_k\delta_{k-I+1}^{-1}g_{k-I+1}, \quad \zeta_k = f_k - \gamma_k\delta_{k-1}^{-1}g_{k-1}, \quad \eta_k = g_k \end{aligned} \tag{4.4.18}$$

Terms that are not defined because an index occurs outside the range $[1, IJ]$ are to be deleted.

From (4.4.18) it follows that **L**, **D** and **U** can overwrite **A**. The only additional storage required is for **N**. Or, if one prefers, elements of **N** can be computed when needed.

Nine-point ILU

The principles are the same as for five- and seven-point ILU. Now the graph $\mathcal{G}$ has nine elements, chosen as follows

$$\mathcal{G} = \mathcal{G}_1 \cup \{(k, k \pm I \pm 1)\} \tag{4.4.19}$$

with $\mathcal{G}_1$ given by (4.4.14). Let the graph of **A** be included in $\mathcal{G}$, and let us write for brevity:

$$z_k = a_{k,k-I-1}, \quad a_k = a_{k,k-I}, \quad b_k = a_{k,k-I+1}, \quad c_k = a_{k,k-1} \quad d_k = a_{kk}$$
$$q_k = a_{k,k+1}, \quad f_k = a_{k,k+I-1}, \quad g_k = a_{k,k+I}, \quad p_k = a_{k,k+I+1} \tag{4.4.20}$$

The structure of the stencil of **A** is as in Figure 3.4.2(c). Let the elements of **L**, **D** and **U** be called ω_k, α_k, β_k, γ_k, δ_k, μ_k, ζ_k, η_k and τ_k. Their locations are identical to those of $z_k, \ldots, p_k$, respectively. Using the same notational conventions as before, one obtains

$$\mathbf{L}\mathbf{D}^{-1}\mathbf{U} = \omega + \alpha + \beta + \gamma + \delta + \mu + \zeta + \eta + \tau + (\omega + \alpha + \beta + \gamma)\delta^{-1}(\mu + \zeta + \eta + \tau) \tag{4.4.21}$$

From (4.4.4) one obtains, with modification:

$$\omega = z, \quad \alpha + \omega\delta^{-1}\mu = a, \quad \beta + \alpha\delta^{-1}\mu = b, \quad \gamma + \omega\delta^{-1}\eta + \alpha\delta^{-1}\zeta = c$$
$$\delta + \omega\delta^{-1}\tau + \alpha\delta^{-1}\eta + \beta\delta^{-1}\zeta + \gamma\delta^{-1}\mu = d + \sigma\tilde{d}, \quad \mu + \alpha\delta^{-1}\tau + \beta\delta^{-1}\eta = q$$
$$\zeta + \gamma\delta^{-1}\eta = f, \quad \eta + \gamma\delta^{-1}\tau = g, \quad \tau = p \tag{4.4.22}$$

The error matrix is given by

$$\mathbf{N} = \omega\delta^{-1}\zeta + \beta\delta^{-1}\mu + \beta\delta^{-1}\tau + \gamma\delta^{-1}\zeta + \sigma\tilde{d} \tag{4.4.23}$$

so that its only non-zero elements are

$$n_{k,k-I+2} = \beta_k\delta_{k-I+1}^{-1}\mu_{k-I+1}, \quad n_{k,k-2} = \omega_k\delta_{k-I-1}^{-1}\zeta_{k-I-1}$$
$$n_{k,k+2} = \beta_k\delta_{k-I+1}^{-1}\tau_{k-I+1}, \quad n_{k,k+I-2} = \gamma_k\delta_{k-1}^{-1}\zeta_{k-1} \tag{4.4.24}$$
$$\sigma\tilde{d}_k = n_{kk} = \sigma \sum_{j \neq k} |n_{kj}|$$

From (4.4.22) we obtain the following recursion

$$\omega_k = z_k, \quad \alpha_k = a_k - \omega_k\delta_{k-I-1}^{-1}\mu_{k-I-1}, \quad \beta_k = b_k - \alpha_k\delta_{k-I}^{-1}\mu_{k-I}$$
$$\gamma_k = c_k - \omega_k\delta_{k-I-1}^{-1}\eta_{k-I-1} - \alpha_k\delta_{k-I}^{-1}\zeta_{k-I},$$
$$\delta_k = d_k - \omega_k\delta_{k-I-1}^{-1}\tau_{k-I-1} - \alpha_k\delta_{k-I}^{-1}\eta_{k-I} - \beta_k\delta_{k-I+1}^{-1}\zeta_{k-I+1} - \gamma_k\delta_{k-1}^{-1}\mu_{k-1} + n_{kk}$$
$$\mu_k = q_k - \alpha_k\delta_{k-I}^{-1}\tau_{k-I} - \beta_k\delta_{k-I+1}^{-1}\eta_{k-I+1}, \quad \zeta_k = f_k - \gamma_k\delta_{k-1}^{-1}\eta_{k-1}$$
$$\eta_k = g_k - \gamma_k\delta_{k-1}^{-1}\tau_{k-1}, \quad \tau_k = p_k \tag{4.4.25}$$

Terms in which an index outside the range $[1, IJ]$ occurs are to be deleted. Again, **L D** and **U** can overwrite **A**.

Alternating ILU

Alternating ILU consists of one ILU iteration of the type just discussed or similar, followed by a second ILU iteration based on a different ordering of the grid points. As an example, alternating seven-point ILU will be discussed. Let the grid be defined by (4.3.1), and let the grid points be numbered according to

$$k = IJ + 1 - j - (i-1)J \tag{4.4.26}$$

This ordering is illustrated in Figure 4.4.1, and will be called here the second backward ordering, to distinguish it from the backward ordering defined by (4.3.3). The ordering (4.4.26) will turn out to be preferable in applications to be discussed in Chapter 7.

Let the graph of **A** be included in $\mathcal{G}$ defined by (4.4.14), and write for brevity $a_k = a_{k,k+1}$, $b_k = a_{k,k-J+1}$, $c_k = a_{k,k+J}$, $d_k = a_{kk}$, $q_k = a_{k,k-J}$, $f_k = a_{k,k+J-1}$, $g_k = a_{k,k-1}$. To distinguish the resulting decomposition from the one obtained with the standard ordering, the factors are denoted by $\bar{\mathbf{L}}$, $\bar{\mathbf{D}}$ and $\bar{\mathbf{U}}$. Let the graph of the incomplete factorization be defined by (4.4.14), and let the elements of $\bar{\mathbf{L}}$, $\bar{\mathbf{D}}$ and $\bar{\mathbf{U}}$ be called $\bar{\alpha}_k$, $\bar{\beta}_k$, $\bar{\gamma}_k$, $\bar{\delta}_k$, $\bar{\mu}_k$, $\bar{\zeta}_k$ and $\bar{\eta}_k$, with locations identical to those of q_k, b_k, g_k, d_k, a_k, f_k and c_k, respectively. Note that, as before, $\bar{\alpha}_k$, $\bar{\beta}_k$, $\bar{\gamma}_k$ and $\bar{\delta}_k$ are elements of $\bar{\mathbf{L}}$, $\bar{\delta}_k$ of $\bar{\mathbf{D}}$, and $\bar{\delta}_k$, $\bar{\mu}_k$, $\bar{\zeta}_k$ and $\bar{\eta}_k$ of $\bar{\mathbf{U}}$. For $\bar{\mathbf{L}}\bar{\mathbf{D}}^{-1}\bar{\mathbf{U}}$ one obtains (4.4.15), and from (4.4.4) it

17	13	9	5	1
18	14	10	6	2
19	15	11	7	3
20	16	12	8	4

Figure 4.4.1 Illustration of second backward ordering.

follows that, with modification,

$$\bar{\alpha} = q, \quad \bar{\beta} + \bar{\alpha}\bar{\delta}^{-1}\bar{\mu} = b, \quad \bar{\gamma} + \bar{\alpha}\bar{\delta}^{-1}\bar{\zeta} = g$$
$$\bar{\delta} + \bar{\alpha}\bar{\delta}^{-1}\bar{\eta} + \bar{\beta}\bar{\delta}^{-1}\bar{\zeta} + \bar{\gamma}\bar{\delta}^{-1}\bar{\mu} = d + \sigma\tilde{d}, \quad \bar{\mu} + \bar{\beta}\bar{\delta}^{-1}\bar{\eta} = a \qquad (4.4.27)$$
$$\bar{\zeta} + \bar{\gamma}\bar{\delta}^{-1}\bar{\eta} = f, \quad \bar{\eta} = c$$

The error matrix is given by $\bar{\mathbf{N}} = \bar{\beta}\bar{\delta}^{-1}\bar{\mu} + \bar{\gamma}\bar{\delta}^{-1}\bar{\zeta} + \sigma\tilde{d}$, so that its only non-zero elements are

$$\bar{n}_{k,k-J+2} = \bar{\beta}_k\bar{\delta}_{k-J+1}^{-1}\bar{\mu}_{k-J+1}, \quad \bar{n}_{k,k+J-2} = \bar{\gamma}_k\bar{\delta}_{k-1}^{-1}\bar{\zeta}_{k-1}$$
$$\sigma\tilde{d} = \bar{n}_{kk} = \sigma(|\bar{n}_{k,k-J+2}| + |\bar{n}_{k,k+J-2}|). \qquad (4.4.28)$$

From (4.4.27) the following recursion is obtained

$$\bar{\alpha}_k = \bar{q}_k, \quad \bar{\beta}_k = b_k - q_k\bar{\delta}_{k-J}^{-1}\bar{\mu}_{k-J}, \quad \bar{\gamma}_k = g_k - \bar{\mu}_k\bar{\delta}_{k-J}^{-1}\bar{\zeta}_{k-J}$$
$$\bar{\delta}_k = d_k - q_k\bar{\delta}_{k-J}^{-1}c_{k-J} - \bar{\beta}_k\bar{\delta}_{k-J+1}^{-1}\bar{\zeta}_{k-J+1} - \bar{\gamma}_k\bar{\delta}_{k-1}^{-1}\bar{\mu}_{k-1} + n_{kk} \qquad (4.4.29)$$
$$\bar{\mu}_k = a_k - \bar{\beta}_k\bar{\delta}_{k-J+1}^{-1}c_{k-J+1}, \quad \bar{\zeta}_k = f_k - \bar{\gamma}_k\bar{\delta}_{k-1}^{-1}c_{k-1}, \quad \bar{\eta}_k = c_k$$

Terms that are not defined because an index occurs outside the range $[1, IJ]$ are to be deleted. From (4.4.29) it follows that $\bar{\mathbf{L}}$, $\bar{\mathbf{D}}$ and $\bar{\mathbf{U}}$ can overwrite $\mathbf{A}$. If, however, alternating ILU is used, $\mathbf{L}$, $\mathbf{D}$ and $\mathbf{U}$ are already stored in the place of $\mathbf{A}$, so that additional storage is required for $\bar{\mathbf{L}}$, $\bar{\mathbf{D}}$ and $\bar{\mathbf{U}}$. $\bar{\mathbf{N}}$ can be stored, or is easily computed, as one prefers.

General ILU

Other ILU variants are obtained for the other choices of $\mathcal{G}$. See Meijerink and van der Vorst (1981) for some possibilities. In general it is advisable to choose $\mathcal{G}$ equal to or slightly larger than the graph of $\mathbf{A}$. If $\mathcal{G}$ is smaller than the graph of $\mathbf{A}$ then nothing changes in the algorithms just presented, except that the elements of $\mathbf{A}$ outside $\mathcal{G}$ are subtracted from $\mathbf{N}$.

The following algorithm (Wesseling (1982a) computes an ILU factorization for general $\mathcal{G}$ by incomplete Gauss elimination. $\mathbf{A}$ is an $n \times n$ matrix. We choose $\text{diag}(\mathbf{L}) = \text{diag}(\mathbf{U})$.

Algorithm 1. Incomplete Gauss elimination

$\mathbf{A}^0 := \mathbf{A}$
for $r := 1$ **step** 1 **until** n **do**
begin $a_{rr}^r := \text{sqrt}\,(a_{rr}^{r-1})$
  for $j > r \wedge (r, j) \in \mathcal{G}$ **do** $a_{rj}^r := a_{rj}^{r-1}/a_{rr}^r$
  for $i > r \wedge (i, r) \in \mathcal{G}$ **do** $a_{ir}^r := a_{ir}^{r-1}/a_{rr}^r$
  for $(i, j) \in \mathcal{G} \wedge i > r \wedge j > r \wedge (i, r) \in \mathcal{G} \wedge (r, j) \in \mathcal{G}$ **do**
  $a_{ij}^r := a_{ij}^{r-1} - a_{ir}^r a_{rj}^r$
  od od od
end of algorithm 1.

$\mathbf{A}^n$ contains $\mathbf{L}$ and $\mathbf{U}$. Hackbusch (1985) gives an algorithm for the $\mathbf{LD}^{-1}\mathbf{U}$ version of ILU, for arbitrary $\mathcal{G}$. See Wesseling and Sonneveld (1980) and Wesseling (1984) for applications of ILU with a fairly complicated $\mathcal{G}$ (Navier–Stokes equations in the vorticity–stream function formulation).

Final remarks

Existence of ILU factorizations and numerical stability of the associated algorithms has been proved by Meijerink and Van der Vorst (1977) if $\mathbf{A}$ is an M-matrix; it is also shown that the associated splitting is regular, so that ILU converges according to Theorem 4.2.3. For information on efficient implementations of ILU on vector and parallel computers, see Hemker *et al.* (1984), Hemker and de Zeeuw (1985), Van der Vorst (1982, 1986, 1989, 1989a), Schlichting and Van der Vorst (1989) and Bastian and Horton (1990).

Exercise 4.4.1. Derive algorithms to compute symmetric ILU factorizations $\mathbf{A} = \mathbf{LD}^{-1}\mathbf{L}^T - \mathbf{N}$ and $\mathbf{A} = \mathbf{LL}^T - \mathbf{N}$ for $\mathbf{A}$ symmetric. See Meijerink and Van der Vorst (1977).

Exercise 4.4.2. Let $\mathbf{A} = \mathbf{L} + \mathbf{D} + \mathbf{U}$, with $\mathbf{D} = \text{diag}(\mathbf{A})$, $l_{ij} = 0$, $j > i$ and $u_{ij} = 0$, $j < i$. Show that (4.4.3) results in symmetric point Gauss–Seidel (cf. Exercise 4.3.1). This shows that symmetric point Gauss–Seidel is a special instance of incomplete point factorization.

4.5. Examples of basic iterative methods: incomplete block LU factorization

Complete line LU factorization

The basic idea of *incomplete block LU-factorization* (IBLU) (also called incomplete line LU-factorization (ILLU) in the literature) is presented by means of the following example. Let the stencil of the difference equations to be solved be given by Figure 3.4.2(c). The grid point ordering is given by (4.3.2). Then the matrix $\mathbf{A}$ of the system to be solved is as follows:

$$\mathbf{A} = \begin{pmatrix} \mathbf{B}_1 & \mathbf{U}_1 & & & & \\ \mathbf{L}_2 & \mathbf{B}_2 & \mathbf{U}_2 & & & \\ & \ddots & \ddots & \ddots & & \\ & & \ddots & \ddots & \mathbf{U}_{J-1} & \\ & & & \mathbf{L}_J & \mathbf{B}_J & \end{pmatrix} \qquad (4.5.1)$$

with $\mathbf{L}_j$, $\mathbf{B}_j$ and $\mathbf{U}_j$ $I \times I$ tridiagonal matrices.

results. Again, $n = 64$ and $\beta = k\pi/12$, $k = 0, 1, 2, \ldots, 23$; Table 7.7.7 gives results only for the worst case in β.

We will not analyse these results further. Numerically we find that for $\beta = 0$ and $\varepsilon \ll 1$ that $\rho = \lambda(0, \pi/2) = (1 + P_1)/(9 + 3P_1) \simeq 1/3$. As $\varepsilon \downarrow 0$, ρ_D depends on the value of $n\varepsilon$. It is clear that we have a robust smoother.

We may conclude that alternating symmetric line Gauss–Seidel is robust for both test problems, provided the mixed derivative is discretized according to (7.5.11). A disadvantage of this smoother is that it does not lend itself to vectorized or parallel computing.

The Jacobi-type methods discussed earlier and Gauss–Seidel with pattern orderings (white–black, zebra) are more favourable in this respect. Fourier smoothing analysis of Gauss–Seidel with pattern orderings is more involved, and is postponed to a later section.

Exercise 7.7.1. Show that damped point Gauss–Seidel is not robust for the rotated anisotropic diffusion equation with $c = 1$, $s = 0$, with standard coarsening.

Exercise 7.7.2. As Exercise 7.7.1, but for the Gauss–Seidel–Jacobi method.

7.8. Incomplete point LU smoothing

For Fourier analysis it is necessary that [**M**] and [**N**] are constant, i.e. do not depend on the location in the grid. For the methods just discussed this is the case if [**A**] is constant. For incomplete factorization smoothing methods this is not, however, sufficient. Near the boundaries of the domain [**M**] (and hence [**N**] = [**M**] − [**A**]) varies, usually tending rapidly to a constant stencil away from the boundaries. Nevertheless, useful predictions about the smoothing performance of incomplete factorization smoothing can be made by means of Fourier analysis. How this can be done is best illustrated by means of an example.

Five-point ILU

This incomplete factorization has been defined in Section 4.4, in standard matrix notation. In Section 4.4 **A** was assumed to have a five-point stencil. With application to test problem (7.5.9) in mind, **A** is assumed to have the seven-point stencil given below. In stencil notation we have

$$[\mathbf{A}] = \begin{bmatrix} f & g & \\ c & d & q \\ & a & b \end{bmatrix}, \quad [\mathbf{L}]_i = \begin{bmatrix} & 0 & \\ c & \delta_i & 0 \\ & a & \end{bmatrix}$$
$$[\mathbf{D}]_i = \begin{bmatrix} & 0 & \\ 0 & \delta_i & 0 \\ & 0 & \end{bmatrix}, \quad [\mathbf{U}]_i = \begin{bmatrix} & g & \\ 0 & \delta_i & q \\ & 0 & \end{bmatrix} \tag{7.8.1}$$

where $i = (i_1, i_2)$. We will study the unmodified version. For δ_i we have the recursion (4.4.12) with $\sigma = 0$:

$$\delta_i = d - ag/\delta_{i-e_2} - cq/\delta_{i-e_1} \tag{7.8.2}$$

where $e_1 = (1, 0)$, $e_2 = (0, 1)$. Terms involving negative values of i_α, $\alpha = 1$ or 2, are to be replaced by zero. We will show the following Lemma.

Lemma 7.8.1. If

$$a + c + d + q + g \geqslant 0, \quad a, c, q, g \leqslant 0, \quad d > 0 \tag{7.8.3}$$

then

$$\lim_{i_1, i_2 \to \infty} \delta_i = \delta \equiv d/2 + [d^2/4 - (ag + cq)]^{1/2} \tag{7.8.4}$$

The proof will be given later. Note that (7.8.3) is satisfied if $b = f = 0$ and **A** is a K-matrix (Section 4.2). Obviously, δ is real, and $\delta \leqslant d$. The rate at which the limit is reached in (7.8.4) will be studied shortly. A sufficient number of mesh points away from the boundaries of the grid G we have approximately $\delta_i = \delta$, and replacing δ_i by δ we obtain for [**M**] = [**L**] [**D**$^{-1}$] [**U**]:

$$[\mathbf{M}] = \begin{bmatrix} cg/\delta & g & \\ c & d & q \\ & a & aq/\delta \end{bmatrix} \tag{7.8.5}$$

and standard Fourier smoothing analysis can be applied. Equation (7.8.5) is derived easily by noting that in stencil notation $(\mathbf{ABu})_i = \sum_j \sum_k \mathbf{A}(i, j)\mathbf{B}(i + j, k)u_{i+j+k}$, so that $\mathbf{A}(i, j)\mathbf{B}(i + j, k)$ gives a contribution to $\mathbf{C}(i, j + k)$, where $\mathbf{C} = \mathbf{AB}$; by summing all contributions one obtains $\mathbf{C}(i, l)$. An explicit expression for $\mathbf{C}(i, l)$ is $\mathbf{C}(i, l) = \sum_j \mathbf{A}(i, j)\mathbf{B}(i + j, l - j)$, since one can write $(\mathbf{Cu})_i = \sum_l \sum_j \mathbf{A}(i, j)\mathbf{B}(i + j, l - j)u_{i+l}$.

Behaviour of elements of L, D, U away from grid boundaries

Before proving Lemma 7.8.1 we prove a preliminary lemma. For brevity we write (j, k) instead of (i_1, i_2).

Lemma 7.8.2. If (7.8.3) is satisfied, then

$$\delta \leqslant \delta_{jk} \leqslant \delta_{j-1,k}, \quad \delta \leqslant \delta_{jk} \leqslant \delta_{j,k-1} \tag{7.8.6}$$

Proof. We have $\delta_{00} = d$, $\delta_{10} = d - cq/d \leqslant \delta_{00}$. Define $\delta_x = d/2 + (d^2/4 - cq)^{1/2}$. Hence $\delta_x \leqslant d$, and $\delta_x = d - cq/\delta_x$, so that $\delta_{10} \geqslant \delta_x$. Assuming $\delta_x \leqslant \delta_{j0} \leqslant \delta_{j-1,0}$ we see that $\delta_{j+1,0} = d - cq/\delta_{j0} \geqslant d - cq/\delta_x = \delta_x$, and $\delta_{j+1,0} \leqslant \delta_{j0}$. In the same

way one can show $\delta_y \leqslant \delta_{0k} \leqslant \delta_{0,k-1}$, with $\delta_y = d/2 + (d^2/4 - ag)^{1/2}$. Since $\delta_x, \delta_y \geqslant \delta$ we have established for $s = 0$:

$$\delta \leqslant \delta_{js} \leqslant \delta_{j-1,s}, \quad \forall j > s; \quad \delta \leqslant \delta_{sk} \leqslant \delta_{s,k-1}, \quad \forall k > s \tag{7.8.7}$$

In the same way it is easy to show for $s = 1$:

$$\delta \leqslant \delta_{js} \leqslant \delta_{j-1,s}, \quad \forall j \geqslant s; \quad \delta \leqslant \delta_{sk} \leqslant \delta_{s,k-1}, \quad \forall k \geqslant s. \tag{7.8.8}$$

By induction it is easy to establish (7.8.8) for arbitrary s. □

Proof of Lemma 7.8.1. According to Lemma 7.8.2, the sequence $\{\delta_{jk}\}$ is non-increasing and bounded from below, and hence converges. The limit Δ satisfies $\Delta \geqslant \delta$, and $\Delta = d - (ag + cq)/\Delta$. Hence $\Delta = \delta$. □

Lemmas 7.8.1 and 7.8.2 are also to be found in Wittum (1989c).

Smoothing factor of five-point ILU

The modified version of incomplete factorization will be studied. As remarked by Wittum (1989a) modification is better than damping, because if the error matrix $\mathbf{N}$ is small with $\sigma = 0$ it will also be small with $\sigma \neq 0$. The optimum σ depends on the problem. A fixed σ for all problems is to be preferred. From the analysis and experiments of Wittum (1989a, 1989c) and our own experiments it follows that $\sigma = 0.5$ is a good choice for all point-factorizations considered here and all problems. Results will be presented with $\sigma = 0$ and $\sigma = 0.5$. The modified version of the recursion (4.4.12) for δ_k is

$$\delta_k = d - ag/\delta_{k-1} - cq/\delta_{k-1} + \sigma\{|\, aq/\delta_{k-1} - b\,| + |\, cg/\delta_{i-1} - f\,|\} \tag{7.8.9}$$

The limiting value δ in the interior of the domain, far from the boundaries, satisfies (7.8.9) with the subscripts omitted, and is easily determined numerically by the following recursion

$$\delta_{k+1} = d - (aq + cq)/\delta_k + \sigma\{|\, aq/\delta_k - b\,| + |\, cg/\delta_k - f\,|\} \tag{7.8.10}$$

The amplification factor is given by

$$\begin{aligned}\lambda(\theta) = \{&(aq/\delta - b)\exp[\mathrm{i}(\theta_1 - \theta_2)] + (cg/\delta - f)\exp[\mathrm{i}(\theta_2 - \theta_1)] + \sigma p\}/\\ &\{a\,\exp(-\mathrm{i}\theta_2) + aq\,\exp[\mathrm{i}(\theta_1 - \theta_2)]/\delta + c\,\exp(-\mathrm{i}\theta_1) + d + \sigma p\\ &+ q\,\exp(\mathrm{i}\theta_1) + cg\,\exp[\mathrm{i}(\theta_2 - \theta_1)]/\delta + g\,\exp(\mathrm{i}\theta_2)\}\end{aligned} \tag{7.8.11}$$

where $p = |\, aq/\delta - b\,| + |\, cg/\delta - f\,|$.

Anisotropic diffusion equation

For the (non-rotated $\beta = 0^0$) anisotropic diffusion equation with discretization (7.5.9) we have $g = a = -1$, $c = q = -\varepsilon$, $d = 2 + 2\varepsilon$, $b = f = 0$, and we obtain: $\delta = 1 + \varepsilon + [2\varepsilon(1 + \sigma)]^{1/2}$, and

$$\begin{aligned}\lambda(\theta) = &[\varepsilon\cos(\theta_1 - \theta_2)/\delta + \sigma\varepsilon/\delta]\,/\\ &[1 + \varepsilon + \sigma\varepsilon/\delta - \varepsilon\cos\theta_1 - \cos\theta_2 + \varepsilon\cos(\theta_1 - \theta_2)/\delta]\end{aligned} \tag{7.8.12}$$

We will study a few special cases. For $\varepsilon = 1$ and $\sigma = 0$ we find in Example 7.8.1:

$$\bar{\rho} = |\,\lambda(\pi/2, -\pi/3)\,| = (2\sqrt{3} + \sqrt{6} - 1)^{-1} \simeq 0.2035 \tag{7.8.13}$$

The case $\varepsilon = 1$, $\sigma \neq 0$ is analytically less tractable. For $\varepsilon \ll 1$ we find in Example 7.8.1:

$$\begin{aligned}0 \leqslant \sigma < 1/2: &\quad \bar{\rho} \simeq |\,\lambda(\pi, 0)\,| = (1 - \sigma)/(2\delta - 1 + \sigma)\\ 1/2 \leqslant \sigma \leqslant 1: &\quad \bar{\rho} \simeq |\,\lambda(\pi/2, 0)\,| = \sigma/(\sigma + \delta)\end{aligned} \tag{7.8.14}$$

$$\begin{aligned}0 \leqslant \sigma < 1/2: &\quad \rho_D \simeq |\,\lambda(\pi, \tau)\,| = (1 - \sigma)/(2\delta - 1 + \sigma + \delta\tau^2/2\varepsilon)\\ 1/2 \leqslant \sigma \leqslant 1: &\quad \rho_D \simeq |\,\lambda(\pi/2, \tau)\,| = (\sigma + \tau)/(\sigma + \delta + \delta\tau^2/2\varepsilon)\end{aligned} \tag{7.8.15}$$

where $\tau = 2\pi/n_2$. These analytical results are confirmed by Table 7.8.1. For example, for $\varepsilon = 10^{-3}$, $n_2 = 64$ and $\sigma = 1/2$ equation (7.8.15) gives $\rho_D \cong 0.090$, $\bar{\rho} \cong 1/3$. Table 7.8.1 includes the worst case for β in the set $\{\beta = k\pi/12, k = 0, 1, 2, \ldots, 23\}$.

Table 7.8.1. Fourier smoothing factors, ρ, ρ_D for the rotated anisotropic diffusion equation discretized according to (7.5.9); five-point ILU smoothing; $n = 64$. In the cases marked with *, $\beta = 45^\circ$

ε	σ	ρ $\beta = 0^\circ, 90^\circ$	ρ $\beta = 15^\circ$	ρ_D $\beta = 0^\circ, 90^\circ$	ρ_D $\beta = 15^\circ$
1	0	0.20	0.20	0.20	0.20
10^{-1}	0	0.48	1.48	0.46	1.44
10^{-2}	0	0.77	7.84	0.58	6.90
10^{-3}	0	0.92	13.0	0.16	10.8
10^{-5}	0	0.99	13.9	0.002	11.5
1	0.5	0.20	0.20	0.20	0.20
10^{-1}	0.5	0.26	0.78*	0.26	0.78*
10^{-2}	0.5	0.30	1.06	0.025	1.01
10^{-3}	0.5	0.32	1.25	0.089	1.18
10^{-5}	0.5	0.33	1.27	0.001	1.20

Here we have another example showing that the influence of the type of the boundary conditions on smoothing analysis may be important. For the non-rotated anisotropic diffusion equation ($\beta = 0^0$ or $\beta = 90^0$) we have a robust smoother both for $\sigma = 0$ and $\sigma = 1/2$, provided the boundary conditions are of Dirichlet type at those parts of the boundary that are perpendicular to the direction of strong coupling. When β is arbitrary, five-point ILU is not a robust smoother with $\sigma = 0$ or $\sigma = 1/2$. We have not experimented with other values of σ, because, as it will turn out, there are other smoothers that are robust, with a fixed choice of σ, that does not depend on the problem.

Example 7.8.1. Derivation of (7.8.13) to (7.8.15). It is easier to work with $1/\lambda$ than with λ. We can write $1/\lambda(\theta) = 1 + \delta\nu(\theta_1, \psi)$ with

$$\nu(\theta_1, \psi) = [1 + \varepsilon - \varepsilon \cos\theta_1 - \cos(\theta_1 - \psi)]/[\varepsilon \cos\psi + \varepsilon\sigma]$$

where $\psi = \theta_1 - \theta_2$. From $\partial\nu/\partial\theta_1 = 0$ it follows that $\varepsilon \sin\theta_1 + \sin\theta_2 = 0$. With $\varepsilon = 1$ this gives $\theta_2 = -\theta_1$ or $\theta_2 = \theta_1 + \pi$. Taking $\sigma = 0$ one finds $1/\lambda(\theta_1, \theta_1 + \pi) = 1 - 2\delta$. Furthermore, $\nu(\theta_1, -\theta_1) = 2(1 - \cos\theta_1)/\cos 2\theta_1$. Extrema of this function are to be found in $\theta_1 = 0, \theta^*, \pi$ where $\theta^* = \cos^{-1}(1 - \sqrt{1/2}) \simeq 73^\circ$. Note that $(0, 0)$ and $(\theta^*, -\theta^*)$ are not in $\bar{\Theta}_r$. Further extrema are to be found on the boundaries of $\bar{\Theta}_r$. For example, $\nu(\pi/2, \theta_2) = (2 - \cos\theta_2)/\sin\theta_2$, which has extrema in $\theta_2 = \pm\pi/3$. Inspection of all extrema on the boundary of $\bar{\Theta}_r$ results in (7.8.13). Continuing with $\varepsilon \ll 1$ and $0 \leqslant \sigma \leqslant 1$, from $\varepsilon \sin\theta_1 + \sin\theta_2 = 0$ found above we have $\theta_2 \simeq 0, \pi$. One finds $\nu(\theta_1, 0) = -1 + (\sigma + 1)/(\sigma + \cos\theta_1)$, which has extrema in $\theta_1 = 0, \pi$. Hence, all extrema in $\bar{\Theta}_r$ are on the boundary of $\bar{\Theta}_r$. We have $\delta \simeq 1$, so that $|1/\lambda(\theta)| \simeq |1 + \nu(\theta)|$. Inspection of the extrema leads to (7.8.14). The extrema in Θ_r^D are expected to be close to those in $\bar{\Theta}_r$, and hence are to be expected in $(\pi, \pm\tau)$, $\tau = 2\pi/n_2$, for $0 \leqslant \sigma < 1/2$, and $(\pi/2, \pm\tau)$ for $1/2 \leqslant \sigma \leqslant 1$. This gives us (7.8.15).

Convection–diffusion equation

Let us take $P_1 = -\alpha P_2$, $\alpha > 0$, $P_2 > 0$, where $P_1 = ch/\varepsilon$, $P_2 = sh/\varepsilon$. Then we have for the convection–diffusion equation discretized according to (7.5.14): $a = -1 - P_2$, $b = f = 0$, $c = -1$, $d = 4 + (1 + \alpha)P_2$, $q = -1 - \alpha P_2$, $g = -1$. After some manipulation one finds that if $\alpha \ll 1$, $P_2 \gg 1$, $\alpha P_2 \gg 1$, then $\lambda(\pi/2, 0) \to i$ as $P_2 \to \infty$. This is in accordance with Table 7.8.2. The worst case obtained when β is varied according to $\beta = k\pi/12$, $k = 0, 1, 2, \ldots, 23$ is listed. Clearly, five-point ILU is not robust for the convection–diffusion equation, at least for $\sigma = 0$ and $\sigma = 0.5$.

Seven-point ILU

Seven-point ILU tends to be more efficient and robust than five-point ILU.

Table 7.8.2. Fourier smoothing factors ρ, ρ_D for the convection–diffusion equation discretized according to (7.5.14); five-point ILU smoothing; $n = 64$

ε	ρ	ρ_D	β	ρ	ρ_D
	$\sigma = 0$			$\sigma = 0.5$	
1	0.20	0.20	0°	0.20	0.20
10^{-1}	0.21	0.21	0°	0.20	0.20
10^{-2}	0.24	0.24	120°	0.24	0.24
10^{-3}	0.60	0.60	105°	0.48	0.48
10^{-5}	0.77	0.71	105°	0.59	0.58

Assume

$$[\mathbf{A}] = \begin{bmatrix} f & g & \\ c & d & q \\ & a & b \end{bmatrix} \tag{7.8.16}$$

The seven-point incomplete factorization $\mathbf{A} = \mathbf{L}\mathbf{D}^{-1}\mathbf{U} - \mathbf{N}$ discussed in Section 4.4 is defined in stencil notation as follows:

$$[\mathbf{L}]_i = \begin{bmatrix} 0 & 0 & \\ \gamma_i & \delta_i & 0 \\ & \alpha_i & \beta_i \end{bmatrix}, \quad [\mathbf{D}]_i = \begin{bmatrix} 0 & 0 & \\ 0 & \delta_i & 0 \\ & 0 & 0 \end{bmatrix}, \quad [\mathbf{U}]_i = \begin{bmatrix} \zeta_i & \eta_i & \\ 0 & \delta_i & \mu_i \\ & 0 & 0 \end{bmatrix} \tag{7.8.17}$$

We have, taking the limit $i \to \infty$ in (4.4.18), assuming the limit exists and writing $\lim_{i\to\infty} \alpha_i = \alpha$ etc.,

$$\begin{aligned} &\alpha = a, \quad \beta = b - a\mu/\delta, \quad \gamma = c - a\zeta/\delta, \\ &\mu = q - \beta g/\delta, \quad \zeta = f - \gamma g/\delta, \quad \eta = g \end{aligned} \tag{7.8.18}$$

with δ the appropriate root of

$$\delta = d - (ag + \beta\zeta + \gamma\mu)\delta + \sigma(|\beta\mu/\delta| + |\gamma\zeta/\delta|) \tag{7.8.19}$$

Numerical evidence indicates that the limiting δ resulting from (4.4.18) as $i \to \infty$ is the same as that for the following recursion, inspired by (4.4.18):

$$\begin{aligned} &\beta_0 = b, \quad \gamma_0 = c, \quad \delta_0 = d, \quad \mu_0 = q, \quad \zeta_0 = f \\ &\beta_{j+1} = b - a\mu_j/\delta_j, \quad \gamma_{j+1} = c - a\zeta_j/\delta_j \\ &\delta_{j+1} = d - (ag + \beta_{j+1}\zeta_j + \gamma_{j+1}\mu_j)/\delta_j + \sigma(|\beta_{j+1}\mu_j/\delta_j| + |\gamma_{j+1}\zeta_j/\delta_j|) \\ &\mu_{j+1} = q - \beta_{j+1}g/\delta_j, \quad \zeta_{j+1} = f - \gamma_{j+1}g/\delta_j \end{aligned} \tag{7.8.20}$$

For $\mathbf{M}$ we find $\mathbf{M} = \mathbf{LD}^{-1}\mathbf{U} = \mathbf{A} + \mathbf{N}$, with

$$[\mathbf{N}] = \begin{bmatrix} p_2 & 0 & 0 & 0 \\ & 0 & p_3 & 0 \\ & 0 & 0 & p_1 \end{bmatrix}, \quad \begin{aligned} p_1 &= \beta\mu/\delta,\ p_2 = \gamma\zeta/\delta, \\ p_3 &= \sigma(|p_1| + |p_2|_1) \end{aligned} \tag{7.8.21}$$

The convergence analysis of (7.8.20) involves greater technical difficulties than the analysis of (7.8.2), and is not attempted.

The amplification factor is given by

$$\begin{aligned} \lambda(\theta) = \{&p_3 + p_1 \exp[\mathrm{i}(2\theta_1 - \theta_2)] + p_2 \exp[-\mathrm{i}(2\theta_1 - \theta_2)]\}/ \\ &\{a \exp(-\mathrm{i}\theta_2) + b \exp[\mathrm{i}(\theta_2 - \theta_1)] + p_1 \exp[\mathrm{i}(2\theta_1 - \theta_2)] + c \exp(-\mathrm{i}\theta_1) \\ &+ d + p_3 + q \exp(\mathrm{i}\theta_1) + p_2 \exp[-\mathrm{i}(2\theta_1 - \theta_2)] \\ &+ f \exp[-\mathrm{i}(\theta_1 - \theta_2)] + g \exp(\mathrm{i}\theta_2)\} \end{aligned} \tag{7.8.22}$$

Anisotropic diffusion equation

For the anisotropic diffusion problem discretized according to (7.5.9) we have symmetry: $\mu = \gamma$, $\zeta = \beta$, $g = a$, $f = b$, $q = c$, so that (7.8.22) becomes

$$\begin{aligned} \lambda(\theta) = &[\sigma p + p \cos(2\theta_1 - \theta_2)]/ \\ &[a \cos\theta_2 + b \cos(\theta_1 - \theta_2) + c \cos\theta_1 + d/2 + \sigma p + p \cos(2\theta_1 - \theta_2)] \end{aligned} \tag{7.8.23}$$

with $p = \beta\mu/\delta$.

With rotation angle $\beta = 90^0$ and $\varepsilon \ll 1$ we find in Example 7.8.2:

$$\begin{aligned} 0 \leqslant \sigma < 1/2: &\quad \bar{\rho} \simeq |\lambda(0, \pi)| \simeq \frac{(1-\sigma)p}{2\varepsilon + \sigma p - p} \\ 1/2 \leqslant \sigma \leqslant 1: &\quad \bar{\rho} \simeq |\lambda(0, \pi/2)| \simeq \frac{\sigma p}{\varepsilon + \sigma p} \end{aligned} \tag{7.8.24}$$

$$\begin{aligned} 0 \leqslant \sigma < 1/2: &\quad \rho_{\mathrm{D}} \simeq |\lambda(\varphi, \pi)| \simeq |(\sigma - 1 + 2\varphi^2)/[\delta^2(2 + \varphi^2/2\varepsilon) + \sigma - 1]| \\ 1/2 \leqslant \sigma \leqslant 1: &\quad \rho_{\mathrm{D}} \simeq |\lambda(\varphi, \pi/2)| \simeq |(\sigma + 2\varphi)/[\delta^2(1 + \varphi^2/2\varepsilon) + \sigma - 2\varphi]| \end{aligned} \tag{7.8.25}$$

with $\varphi = 2\pi/n_1$. These results agree approximately with Table 7.8.3. For example, for $\varepsilon = 10^{-3}$, $n_1 = 64$ equation (7.8.25) gives $\rho_{\mathrm{D}} \simeq 0.152$ for $\sigma = 0$, and $\rho_{\mathrm{D}} \simeq 0.103$ for $\sigma = 0.5$.

Table 7.8.3 includes the worst case for β in the set $\{\beta = k\pi/12, k = 0, 1, 2, \ldots, 23\}$. Equations (7.8.24) and (7.8.25) and Table 7.8.3 show that the boundary conditions may have an important influence. For rotation angle $\beta = 0$ or $\beta = 90^\circ$, seven-point ILU is a good smoother

Table 7.8.3. Fourier smoothing factors ρ, ρ_{D} for the rotated anisotropic diffusion equation discretized according (7.5.9); seven-point ILU smoothing; $n = 64$

ε	σ	ρ $\beta = 0^\circ$	ρ $\beta = 90^\circ$	ρ, β	ρ_{D} $\beta = 0^\circ$	ρ_{D} $\beta = 90^\circ$	ρ_{D}, β
1	0	0.13	0.13	0.13, any	0.12	0.12	0.12, any
10^{-1}	0	0.17	0.27	0.45, 75°	0.16	0.27	0.44, 75°
10^{-2}	0	0.17	0.61	1.35, 75°	0.11	0.45	1.26, 75°
10^{-3}	0	0.17	0.84	1.69, 75°	0.02	0.16	1.55, 75°
10^{-5}	0	0.17	0.98	1.74, 75°	10^{-4}	0.002	1.59, 75°
1	0.5	0.11	0.11	1.11, any	0.11	0.11	0.11, any
10^{-1}	0.5	0.089	0.23	0.50, 60°	0.087	0.23	0.50, 60°
10^{-2}	0.5	0.091	0.27	0.77, 60°	0.075	0.25	0.77, 60°
10^{-3}	0.5	0.091	0.31	0.82, 60°	0.029	0.097	0.82, 60°
10^{-5}	0.5	0.086	0.33	0.83, 60°	4×10^{-4}	10^{-3}	0.82, 60°

for the anisotropic diffusion equation. With $\sigma = 0.5$ we have a robust smoother; finer sampling of β and increasing n gives results indicating that ρ and ρ_{D} are bounded away from 1. For some values of β this smoother is not, however, very effective. One might try other values of σ to diminish ρ_{D}. But we did not find a fixed, problem-independent choice that would do. A more efficient and robust ILU type smoother will be introduced shortly. In Example 7.8.3 it is shown that $\sigma = 1/2$ is optimal for $\beta = 45^0$.

Example 7.8.2. Derivation of (7.8.24) and (7.8.25). This example is similar to Example 7.8.1. We have $a = g = -\varepsilon$, $b = f = 0$, $c = q = -1$, $d = 2 - 2\varepsilon$. Equation (7.8.18) gives $\gamma = -1 + \varepsilon^2\gamma/\delta^2$, hence $\gamma \simeq -1$, $\beta \simeq \varepsilon/\delta$ and $p = \varepsilon/\delta^2$. Furthermore, $\delta \simeq d - (\varepsilon^2 + \varepsilon^2/\delta^2 + 1)/\delta + 2\sigma\varepsilon/\delta^2 \simeq d + 2\sigma\varepsilon - 1/\delta$, so that $\delta \simeq 1 + [(1+\sigma)2\varepsilon]^{1/2}$. Writing $2\theta_1 - \theta_2 = \psi$ we have $\lambda(\theta)^{-1} = 1 + \nu(\theta_1, \psi)$ with $\nu(\theta_1, \psi) = [1 + \varepsilon - \cos\theta_1 - \varepsilon\cos(2\theta_1 - \psi)]/(\sigma p + p\cos\psi)$. From $\partial\nu/\partial\theta_1 = 0$ it follows that $\sin\theta_1 + 2\varepsilon\sin(2\theta_1 - \psi) = 0$. For $\varepsilon \ll 1$ this implies $\theta_1 \simeq 0$ or π. One finds

$$|\lambda(0, \theta_2)| \simeq |(\sigma p + p\cos\theta_2)/(\varepsilon + \sigma p - \varepsilon\cos\theta_2 + p\cos\theta_2)| \geqslant |\lambda(\pi, \theta_2)|$$

and (7.8.24) follows. $\mathrm{Max}\{\lambda(\theta): \theta \in \Theta_{\mathrm{r}}^{\mathrm{D}}\}$ will be reached close so $(\pm\varphi, \pi)$ or $(\pm\varphi, \pi/2)$, and (7.8.25) results.

Example 7.8.3. Show that for $\beta = 45^\circ$ and $\varepsilon \ll 1$

$$\rho \simeq \max\left\{\left|\frac{\sigma - 1}{\sigma + 1}\right|, \left|\frac{\sigma}{\sigma + 1}\right|\right\} \tag{7.8.26}$$

Hence, the optimal value of σ for this case is $\sigma = 0.5$, for which $\rho \simeq 1/3$.

Equation (7.8.26) can be derived as follows. We have $a = c = q = g = -\varepsilon$, $b = f = (\varepsilon - 1)/2$, $d = 3\varepsilon + 1$. Symmetry means that $\mu = \gamma$, $\zeta = \beta$, $\eta = \alpha$. Equations (7.8.18), (7.8.19) and (7.8.21) give: $\alpha = a$, $\beta = b - a\gamma/\delta$, $\gamma = a(1 - \beta/\delta)$, $p_1 = p_2 = p = \beta\gamma/\delta$, $\delta = d - (a^2 + \beta^2 + \gamma^2)/\delta + 2\sigma|p|$. For $\varepsilon \ll 1$ this gives $\beta = -1/2 + \frac{1}{2}\varepsilon + O(\varepsilon^2)$, $\gamma = -2\varepsilon + O(\varepsilon^{3/2})$, $p = 2\varepsilon + O(\varepsilon^{3/2})$, $\delta = \frac{1}{2} + [2(1+\sigma)\varepsilon]^{1/2} + O(\varepsilon)$. With $p \simeq 2\varepsilon$ and keeping only O(1) terms in the (7.5.14) gives $a = -\varepsilon - hs$, $b = 0$, $c = -\varepsilon$, $d = 4\varepsilon - ch + sh$, $q = -\varepsilon + hc$, Hence, $|\lambda(\theta)| \to \infty$ when $\theta_2 \to \theta_1$. The maximum of $|\lambda(\theta)|$ is, therefore, expected to occur for $\theta_2 \simeq \theta_1$, when $O(\varepsilon)$ terms are included in the denominator. Equation (7.8.22) gives $\lambda(\theta_1, \theta_1) \simeq (\cos\theta_1 + \sigma)/(1+\sigma)$. To determine ρ it suffices to consider the set $\theta_1 \in [\pi/2, \pi]$, and (7.8.26) follows.

Convection–diffusion equation

Table 7.8.4 gives some results for the convection–diffusion equation. The worst case for β in the set $\{\beta = k\pi/12: k = 0, 1, 2, \ldots, 23\}$ is listed. It is found numerically that $\rho \ll 1$ and $\rho_D \ll 1$ when $\varepsilon \ll 1$, except for β close to 0° or 180°, where ρ and ρ_D are found to be much larger than for other values of β, which may spell trouble. We, therefore, do some analysis. Numerically it is found that for $\varepsilon \ll 1$ and $|s| \ll 1$ we have $\rho \simeq |\lambda(0, \pi/2)|$, both for $\sigma = 0$ and $\sigma = 1/2$. We proceed to determine $\lambda(0, \pi/2)$. Assume $c < 0$, $s > 0$; then (7.5.14) gives $a = -\varepsilon - hs$, $b = 0$, $c = -\varepsilon$, $d = 4\varepsilon - ch + sh$, $q = -\varepsilon + hc$, $f = 0$, $g = -\varepsilon$. Equations (7.8.18) and (7.8.19) give, assuming $\varepsilon \ll 1$, $|s| \ll 1$ and keeping only leading terms in ε and s, $\beta \simeq (\varepsilon + sh)ch/\delta$, $\gamma \simeq -\varepsilon$, $\mu \simeq ch$, $\zeta \simeq 0$, $\delta \simeq (s - c)h$, $p_1 \simeq (\varepsilon + sh)c^2/(s-c)^2$, $p_2 = 0$. Substitution in (7.8.22) and neglect of a few higher order terms results in

$$\lambda(0, \pi/2) \simeq \frac{(\sigma - i)(\tau + 1)}{(\tau + 2)(1 - 2\tan\beta) + \sigma(1 + \tau) + i(1 - 2\tau\tan\beta)} \tag{7.8.27}$$

Table 7.8.4. Fourier smoothing factors ρ, ρ_D for the convection–diffusion equation discretized according to (7.5.14); seven-point ILU smoothing; $n = 64$

	$\sigma = 0$			$\sigma = 0.5$		
ε	ρ	ρ_D	β	ρ	ρ_D	β
1	0.13	0.12	90°	0.11	0.11	0°
10^{-1}	0.13	0.13	90°	0.12	0.12	0°
10^{-2}	0.16	0.16	0°	0.17	0.17	165°
10^{-3}	0.44	0.43	165°	0.37	0.37	165°
10^{-5}	0.58	0.54	165°	0.47	0.47	165°

where $\tau = sh/\varepsilon$, so that

$$\rho^2 \simeq (\tau+1)^2(\sigma^2+1)/\{[(\tau+2)(1-2\tan\beta) + \sigma(1+\tau)]^2 + (1-2\tau\tan\beta)^2\} \tag{7.8.28}$$

hence,

$$\rho^2 \leqslant (\sigma^2+1)/(\sigma+1)^2 \tag{7.8.29}$$

Choosing $\sigma = 1/2$, (7.8.29) gives $\rho \leqslant \frac{1}{3}\sqrt{5} \simeq 0.75$, so that the smoother is robust. With $\sigma = 0$, inequality (7.8.29) does not keep ρ away from 1. Equation (7.8.28) gives, for $\sigma = 0$:

$$\lim_{\tau\to 0} \rho = 1/\sqrt{5}, \quad \lim_{\tau\to\infty} \rho = (1 - 4\tan\beta + 8\tan^2\beta)^{-1/2} \tag{7.8.30}$$

This is confirmed by numerical experiments. With $\sigma = 1/2$ we have a robust smoother for the convection–diffusion equation. Alternating ILU, to be discussed shortly, may, however, be more efficient. With $\sigma = 0$, $\rho \ll 1$ except in a small neighbourhood of $\beta = 0^\circ$ and $\beta = 180^\circ$. Since in practice τ remains finite, some smoothing effect remains. For example, for $s = 0.1$ ($\beta \simeq 174.3$), $h = 1/64$ and $\varepsilon = 10^{-5}$ we have $\tau \simeq 156$ and (7.8.30) gives $\rho \simeq 0.82$. This explains why in practice seven-point ILU with $\sigma = 0$ is a satisfactory smoother for the convection–diffusion equation but $\sigma = 1/2$ gives a better smoother.

Nine-point ILU

Assume

$$[\mathbf{A}] = \begin{bmatrix} f & g & p \\ c & d & q \\ z & a & b \end{bmatrix} \tag{7.8.31}$$

Reasoning as before, we have

$$[\mathbf{L}] = \begin{bmatrix} 0 & 0 & 0 \\ \gamma & \delta & 0 \\ \omega & \alpha & \beta \end{bmatrix}, \quad \mathbf{D} = \begin{bmatrix} 0 & 0 & 0 \\ 0 & \delta & 0 \\ 0 & 0 & 0 \end{bmatrix}, \quad \mathbf{U} = \begin{bmatrix} \zeta & \eta & \tau \\ 0 & \delta & \mu \\ 0 & 0 & 0 \end{bmatrix} \tag{7.8.32}$$

For $\omega, \alpha, \ldots, \tau$ we have equations (4.4.22), here interpreted as equations for

scalar unknowns. The relevant solution of these equations may be obtained as the limit of the following recursion, inspired by (4.4.25):

$$\begin{gathered}\alpha_0 = a, \quad \beta_0 = b, \quad \gamma_0 = c, \quad \delta_0 = d, \quad \mu_0 = q, \quad \zeta_0 = f, \quad \eta_0 = g \\ \alpha_{j+1} = a - z\mu_j/\delta_j, \quad \beta_{j+1} = b - \alpha_{j+1}\mu_j/\delta_j \\ \gamma_{j+1} = c - (z\eta_j + \alpha_{j+1}\zeta_j)/\delta_j \\ n_{j+1} = \{|\beta_{j+1}\mu_j| + |z\zeta_j| + |\beta_{j+1}p| + |\gamma_{j+1}\zeta_j|\}/\delta_j \\ \delta_{j+1} = d - (zp + \alpha_{j+1}\eta_j + \beta_{j+1}\zeta_j + \gamma_{j+1}\mu_j)/\delta_j + \sigma n_{j+1} \\ \mu_{j+1} = q - (\alpha_{j+1}p + \beta_{j+1}\eta_j)/\delta_{j+1} \\ \zeta_{j+1} = f - \gamma_{j+1}\eta_j/\delta_j, \quad \eta_{j+1} = g - \gamma_{j+1}p/\delta_{j+1}\end{gathered} \tag{7.8.33}$$

For $\mathbf{M}$ we find $\mathbf{M} = \mathbf{L}\mathbf{D}^{-1}\mathbf{U} = \mathbf{A} + \mathbf{N}$, with

$$\mathbf{N} = \frac{1}{8}\begin{bmatrix} \gamma\zeta & 0 & 0 & 0 & \\ z\zeta & 0 & \sigma n & 0 & \beta p \\ & 0 & 0 & 0 & \beta\mu \end{bmatrix} \tag{7.8.34}$$

with $n = |\gamma\zeta| + |z\zeta| + |\beta p| + |\beta\mu|$. The amplification factor is given by

$$\lambda(\theta) = B(\theta)/\{(B(\theta) + A(\theta)\} \tag{7.8.35}$$

where

$$\begin{aligned}B(\theta) = \{&\gamma\zeta \exp[\mathrm{i}(\theta_2 - 2\theta_1)] + z\zeta \exp(-2\mathrm{i}\theta_1) \\ &+ \beta p \exp(2\mathrm{i}\theta_1) + \beta\mu \exp[\mathrm{i}(2\theta_1 - \theta_2] + \sigma n\}/\delta\end{aligned}$$

and

$$\begin{aligned}A(\theta) = z \exp[-\mathrm{i}(\theta_1 + \theta_2)] + a \exp(-\mathrm{i}\theta_2) + b \exp[\mathrm{i}(\theta_1 - \theta_2)] + c \exp(-\mathrm{i}\theta_1) \\ + d + q \exp(\mathrm{i}\theta_1) + f \exp[\mathrm{i}(\theta_2 - \theta_1)] + g \exp(\mathrm{i}\theta_2) + p \exp[\mathrm{i}(\theta_1 + \theta_2)]\end{aligned}$$

Anisotropic diffusion equation

For the anisotropic diffusion equation discretized according to (7.5.9) the nine-point ILU factorization is identical to the seven-point ILU factorization. Table 7.8.5 gives results for the case that the mixed derivative is discretized according to (7.4.11). In this case seven-point ILU performs poorly. When the mixed derivative is absent ($\beta = 0^\circ$ or $\beta = 90^\circ$) nine-point ILU is identical to seven-point ILU. Therefore Table 7.8.5 gives only the worst case for β in the set $\{\beta = k/2\pi, k = 0, 1, 2, \ldots, 23\}$. Clearly, the smoother is not robust for $\sigma = 0$. But also for $\sigma = 1/2$ there are values of β for which this smoother is not

Table 7.8.5. Fourier smoothing factors ρ, ρ_D for the rotated anisotropic diffusion equation discretized according to (7.5.9), but the mixed derivative discretized according to (7.5.11); nine-point ILU smoothing; $n = 64$

	$\sigma = 0$				$\sigma = \frac{1}{2}$			
ε	ρ	β	ρ_D	β	ρ	β	ρ_D	β
1	0.13	any	0.12	any	0.11	any	0.11	any
10^{-1}	0.52	75°	0.50	75°	0.42	75°	0.42	60°
10^{-2}	1.51	75°	1.34	75°	0.63	75°	0.63	75°
10^{-3}	1.87	75°	1.62	75°	0.68	75°	0.68	75°
10^{-5}	1.92	75°	1.66	75°	0.68	75°	0.68	75°

very effective. For example, with finer sampling of β around 75° one finds a local maximum of approximately $\rho_D = 0.73$ for $\beta = 85^\circ$.

Alternating seven-point ILU

The amplification factor of the second part (corresponding to the second backward grid point ordering defined by (4.4.26)) of alternating seven-point ILU smoothing, with factors denoted by $\bar{\mathbf{L}}$, $\bar{\mathbf{D}}$, $\bar{\mathbf{U}}$, may be determined as follows. Let $[\mathbf{A}]$ be given by (7.8.16). The stencil representation of the incomplete factorization discussed in Section 4.4 is

$$[\bar{\mathbf{L}}] = \begin{bmatrix} 0 & \bar{\gamma} & \\ 0 & \bar{\delta} & \bar{\alpha} \\ & 0 & \bar{\beta} \end{bmatrix}, \quad [\bar{\mathbf{D}}] = \begin{bmatrix} 0 & 0 & \\ 0 & \bar{\delta} & 0 \\ & 0 & 0 \end{bmatrix}, \quad \bar{\mathbf{U}} = \begin{bmatrix} \bar{\zeta} & 0 & \\ \bar{\eta} & \bar{\delta} & 0 \\ & \bar{\mu} & 0 \end{bmatrix} \tag{7.8.36}$$

Equation (4.4.27) and (4.4.29) show that $\bar{\alpha}, \bar{\beta}, \ldots, \bar{\eta}$ are given by (7.8.18) and (7.8.19), provided the following substitutions are made:

$$a \to q, \quad b \to b, \quad c \to g, \quad d \to d, \quad q \to a, \quad f \to f, \quad g \to c \tag{7.8.37}$$

The iteration matrix is $\bar{\mathbf{M}} = \bar{\mathbf{L}}\bar{\mathbf{D}}^{-1}\bar{\mathbf{U}} = \mathbf{A} + \bar{\mathbf{N}}$. According to (4.4.28),

$$[\bar{\mathbf{N}}] = \begin{bmatrix} \bar{p}_2 & & \\ 0 & 0 & 0 \\ 0 & \bar{p}_3 & 0 \\ 0 & 0 & 0 \\ & & \bar{p}_1 \end{bmatrix} \tag{7.8.38}$$

with $\bar{p}_1 = \bar{\beta}\bar{\mu}/\bar{\delta}$, $\bar{p}_2 = \bar{\gamma}\bar{\zeta}/\bar{\delta}$, $\bar{p}_3 = \sigma(|\bar{p}_1| + |\bar{p}_2|)$. It follows that the amplification

factor $\tilde{\lambda}(\theta)$ of the second step of alternating seven-point ILU smoothing is given by

$$\tilde{\lambda}(\theta) = \{\tilde{p}_3 + \tilde{p}_1 \exp[i(\theta_1 - 2\theta_2)] + \tilde{p}_2 \exp[i(2\theta_2 - \theta_1)]\}/$$
$$\{a \exp(-i\theta_2) + b \exp[i(\theta_1 - \theta_2)] + c \exp(i\theta_1) + d + \tilde{p}_3 + q \exp(i\theta_1)$$
$$+ f \exp[-i(\theta_1 - \theta_2)] + g \exp(i\theta_2) + \tilde{p}_1 \exp[i(\theta_1 - 2\theta_2)]$$
$$+ \tilde{p}_2 \exp[i(2\theta_2 - \theta_1)]\} \quad (7.8.39)$$

The amplification factor of alternating seven-point ILU is given by $\lambda(\theta)\tilde{\lambda}(\theta)$, with $\lambda(\theta)$ given by (7.8.22).

Anisotropic diffusion equation

Table 7.8.6 gives some results for the rotated anisotropic diffusion equation. The worst case for β in the set $\{\beta = k\pi/12,\ k = 0, 1, 2, \ldots, 23\}$ is included. We see that with $\sigma = 0.5$ we have a robust smoother for this test case. Similar results (not given here) are obtained when the mixed derivative is approximated by (7.5.11) with alternating nine-point ILU.

Table 7.8.6. Fourier smoothing factors ρ, ρ_D for the rotated anisotropic diffusion equation discretized according to (7.5.9); alternating seven-point ILU smoothing; $n = 64$

ε	σ	ρ $\beta = 0°, 90°$	ρ_D $\beta = 0°, 90°$	ρ, ρ_D	β
1	0	9×10^{-3}	9×10^{-3}	9×10^{-3}	any
10^{-1}	0	0.021	0.021	0.061	30°
10^{-2}	0	0.041	0.024	0.25	45°
10^{-3}	0	0.057	3×10^{-3}	0.61	45°
10^{-5}	0	0.064	10^{-6}	0.94	45°
1	0.5	4×10^{-3}	4×10^{-3}	4×10^{-3}	any
10^{-1}	0.5	0.014	0.014	0.028	15°
10^{-2}	0.5	0.020	0.012	0.058	45°
10^{-3}	0.5	0.026	2×10^{-3}	0.090	45°
10^{-5}	0.5	0.028	0	0.11	45°

Convection–diffusion equation

Symmetry considerations, mean that we expect that the second step of alternating seven-point ILU smoothing has, for $\varepsilon \ll 1$, $\rho \simeq 1$ for β around 90° and 270°. Here, however, the first step has $\rho \ll 1$. Hence, we expect the alternating smoother to be robust for the convection–diffusion equation. This is confirmed by the results of Table 7.8.7. The worst case for β in the set $\{\beta = k\pi/12: k = 0, 1, 2, \ldots, 23\}$ is listed.

To sum up, alternating modified point ILU is robust and very efficient in all cases. The use of alternating ILU has been proposed by Oertel and Stüben (1989). Modification has been analyzed and tested by Hemker (1980), Oertel and Stüben (1989), Khalil (1989, 1989a) and Wittum (1989a, 1989c).

Table 7.8.7. Fourier smoothing factors ρ, ρ_D for the convection-diffusion equation discretized according to (7.5.14); alternating seven-point ILU smoothing; $n = 64$

	$\sigma = 0$		$\sigma = 0.5$	
ε	ρ, ρ_D	β	ρ, ρ_D	β
1.0	9×10^{-3}	0°	4×10^{-3}	0°
10^{-1}	9×10^{-3}	0°	4×10^{-3}	0°
10^{-2}	0.019	105°	7×10^{-3}	0°
10^{-3}	0.063	105°	0.027	120°
10^{-5}	0.086	105°	0.036	105°

7.9. Incomplete block factorization smoothing

Smoothing analysis

According to (4.5.8), the iteration matrix $\mathbf{M}$ is given by $\mathbf{M} = (\mathbf{L} + \tilde{\mathbf{D}})\tilde{\mathbf{D}}^{-1}(\tilde{\mathbf{D}} + \mathbf{U})$, with $\mathbf{L}$ and $\mathbf{U}$ parts of $\mathbf{A}$ as defined by (4.5.1) and (4.5.3), and $\tilde{\mathbf{D}}$ a tridiagonal matrix defined by (4.5.3) and (4.5.7). Far enough away from the boundaries the stencil $[\mathbf{M}]$ becomes independent of the grid location, and this stencil must be determined for the application of Fourier smoothing analysis, as before. This can be done as follows.

For brevity, the looked for i-independent values of $\tilde{\mathbf{D}}_{i,i-1}$, $\tilde{\mathbf{D}}_{ii}$ and $\tilde{\mathbf{D}}_{i,i+1}$ are denoted by $\tilde{b}$, $\tilde{a}$, $\tilde{c}$, respectively; those of the triangular factorization (4.5.11) are denoted by $\tilde{e}$, $\tilde{f}$, $\tilde{g}$; and the i-independent values s_{ij} of $\tilde{\mathbf{D}}^{-1}$ in (4.5.13) are denoted by $\tilde{s}_{j-i} = s_{ij}$, those of t_{ij} (elements of tridiag$(\mathbf{L}\tilde{\mathbf{D}}^{-1}\mathbf{U})$ by $\tilde{t}_{j-i} = t_{ij}$. Based on Algorithm 1 of Section 4.5 we find $\tilde{b}$, $\tilde{a}$, $\tilde{c}$ by means of the following iterative method:

Algorithm 1 Computation of $[\tilde{\mathbf{D}}]$
begin $\tilde{b} = c$, $\tilde{a} = d$, $\tilde{c} = q$, $\tilde{f} = 1/\tilde{a}$, $\tilde{g} = \tilde{c}\tilde{f}$
do until convergence
$\tilde{e} = \tilde{b}\tilde{f}$, $\tilde{f} = 1/(\tilde{a} - \tilde{e}\tilde{g}/\tilde{f})$, $\tilde{g} = \tilde{c}\tilde{f}$
$\tilde{s}_0 = \tilde{f}/(1 - \tilde{g}\tilde{e})$, $\tilde{s}_{-1} = -\tilde{e}\tilde{s}_0$, $\tilde{s}_{-2} = -\tilde{e}\tilde{s}_{-1}$, $\tilde{s}_{-3} = -\tilde{e}\tilde{s}_{-2}$
$\tilde{s}_1 = -\tilde{g}\tilde{s}_0$, $\tilde{s}_2 = -\tilde{g}\tilde{s}_1$, $\tilde{s}_3 = -\tilde{g}\tilde{s}_2$
$k = -2, -1, \ldots, 2$: $\sigma_k = z\tilde{s}_{k+1} + a\tilde{s}_k + b\tilde{s}_{k-1}$
$k = -1, 0, 1$: $\tilde{t}_k = f\sigma_{k+1} + g\sigma_k + p\sigma_{k-1}$
$\tilde{b} = c - \tilde{t}_{-1}$, $\tilde{a} = d - \tilde{t}_0$, $\tilde{c} = q - \tilde{t}_1$
od
end